(Preprint) AAS 18-388

STATIONKEEPING, ORBIT DETERMINATION, AND ATTITUDE CONTROL FOR SPACECRAFT IN NEAR RECTILINEAR HALO ORBITS

Clark P. Newman,[*] Diane C. Davis,[†] Ryan J. Whitley,[‡] Joseph R. Guinn,[§] and Mark S. Ryne[**]

From a Near Rectilinear Halo Orbit (NRHO), NASA's Gateway at the Moon is planned to serve as a proving ground and a staging location for human missions beyond Earth. Stationkeeping, Orbit Determination (OD), and attitude control are examined for uncrewed and crewed Gateway configurations. Orbit maintenance costs are investigated using finite maneuvers, considering skipped maneuvers and perturbations. OD analysis assesses DSN tracking and identifies OD challenges associated with the NRHO and crewed operations. The Gateway attitude profile is simulated to determine an effective equilibrium attitude. Attitude control propellant use and sizing of the required passive attitude control system are assessed.

INTRODUCTION

NASA's proposed Gateway near the Moon is planned as part of an evolutionary staging into deep space crewed missions. The Gateway is designed as a proving ground for deep space technologies and a staging ground to facilitate missions to low lunar orbit and the lunar surface as well as to asteroids and Mars. The Gateway is envisioned as a crew-tended spacecraft that will operate in both crewed and uncrewed environments, built up in stages over time. Gateway components may arrive as co-manifested payloads with the Orion spacecraft or they may be launched individually.

To support Gateway goals, a cislunar Near Rectilinear Halo Orbit (NRHO) [1] is currently baselined as the Gateway trajectory. The four NRHO families are subsets of the larger halo families and are characterized by bounded stability properties. The baseline NRHO is an L2 southern halo in a 9:2 resonance with the lunar synodic period. The orbit passes through perilune over the north lunar pole approximately every 6.5 days with a close approach radius of about 3,200 km and an apolune radius of approximately 70,000 km. While the target NRHO exhibits nearly stable characteristics, an uncontrolled spacecraft in the NRHO will eventually depart the vicinity of the Moon. Small orbit maintenance maneuvers (OMM) are required to ensure long-term operations in the NRHO, and the cost of the OMM depends on the quality of the navigation solution available. Solar pressure and the gravity gradient near perilune effect the spacecraft attitude, and moments can be significant, especially on long Gateway stacks. An appropriately sized attitude control system is needed to maintain spacecraft attitude.

[*] Senior Systems Engineer, a.i. solutions, Inc., 2224 Bay Area Blvd, Houston TX 77058.
[†] Principal Systems Engineer, a.i. solutions, Inc., 2224 Bay Area Blvd, Houston TX 77058.
[‡‡] Deputy Systems Integration Manager, Exploration Mission Planning Office, NASA Johnson Space Center, 2101 NASA Parkway, Houston, Texas 77058.
[§§] Manager, Mission Design and Navigation Section, Jet Propulsion Laboratory, California Institute of Technology, 4800 Oak Grove Drive, Pasadena, CA 91109.
[**] Navigation Engineer, Mission Design and Navigation Section, Jet Propulsion Laboratory, California Institute of Technology, 4800 Oak Grove Drive, Pasadena, CA 91109.

In previous studies,[1-4] the process of orbit maintenance (OM) of a spacecraft in an NRHO is investigated using impulsive maneuvers. The current investigation extends the *x*-axis crossing control method detailed previously to incorporate low thrust maneuvers using solar electric propulsion (SEP) for configurations in which long, efficient maneuvers are preferable. Both uncrewed, quiet configurations and crewed, noisy configurations are explored. Docking and undocking perturbations are considered, and the effects of skipping maneuvers during both crewed and uncrewed operations are examined. Significant operational differences between the crewed and uncrewed cases lead to higher costs for stationkeeping during crewed operations.

The cost of orbit maintenance depends heavily on the quality of the orbit determination (OD) available for the Gateway. Gateway OD in the NRHO is explored via linear covariance analysis for ground-based, Deep Space Network (DSN) tracking for both uncrewed and crewed operations. Tracking data schedules are explored in both cases to determine the number of DSN passes required to meet OD requirements. Careful pass placement can help mitigate the effects of added perturbations during crewed operations.

Finally, an attitude control system (ACS) is considered. Attitude control must account for torques due to solar radiation pressure (SRP) and gravity gradient torques near the Moon. It must maintain a solar pressure equilibrium attitude (SPEA) during uncrewed operations and meet tail-to-Sun requirements of the Orion spacecraft during crewed operations. The ACS must also perform slews to orient the Gateway for OMMs. The ACS is defined as control system paired with an angular momentum capacity to emulate reaction wheels or control moment gyros (CMGs) absorbing momentum to maintain a stable attitude. The control system is executed with either RCS thrusters on the Power and Propulsion Element (PPE) of the Gateway or with control torques delivered by reaction wheels or CMGs. The design space is explored to determine attitude control performance, namely to document the use of RCS hydrazine propellant, and to feasible reaction wheel or CMG sizing to handle operations.

BACKGROUND

Near Rectilinear Halo Orbit (NRHO)

The Gateway orbit considered in the current study is an L_2 southern NRHO in a 9:2 resonance with the Lunar synodic period. This orbit is a member of the halo family, a multibody orbit that is heavily influenced by the gravitational attraction of both the Moon and the Earth. The orbit appears in three reference frames in Figure 1. It is quasi-periodic in the Earth-Moon rotating frame, and its resonance is visible in the Moon-centered inertial view. The 9:2 Lunar synodic resonant (LSR) NRHO possesses an orbital period of about 6.5 days, a perilune radius (r_p) of about 3,200 km, and an apolune radius (r_a) of approximately 70,000 km. The orbit is favorable for Gateway operations for several reasons.[5] Transfers from Earth are relatively inexpensive in both the crewed (short, chemical transfers) and uncrewed (long, chemical or SEP transfers) cases.[6] Similarly, low-cost transfers are available from the NRHO to other orbits in Cislunar space, such as other Halo orbits,[7] Distant Retrograde Orbits (DROs),[8] Butterfly Orbits,[4] and Low Lunar Orbits (LLOs).[6] Additionally, NRHOs display nearly stable behavior; orbit maintenance costs are inexpensive, and the trajectory is tolerant to missed maneuvers and perturbations.[3] Also, because the orbit is resonant with the lunar synodic period, the spacecraft can be phased in the orbit such that it avoids eclipses due to the Earth's shadow.[1,9]

Perfectly periodic in the Circular Restricted 3-Body Problem (CR3BP), NRHOs, like other halos, are easily corrected into quasi-periodic orbits in higher fidelity ephemeris force models using a variety of methods.[2,4,9] The current study employs a set of long-horizon reference trajectories that are corrected into the ephemeris model for durations of up to 15 years; the orbit appearing in Figure 1 is an example. The corrected NRHOs retain many of the characteristics of their perfectly periodic CR3BP analogs.

Gateway Configurations

As the Gateway is built up over time and visited by the Orion spacecraft, physical properties will change significantly. Several notional Gateway configurations are considered in the current analysis; each mass appears in Table 1. First, the smallest Gateway stack is considered, denoted configuration 1. It is joined by the crewed Orion carrying a comanifested payload (CMP), configuration 2. Orion then departs with the crew, leaving the CMP behind in configuration 3. A refueling scenario considers the addition of a logistics element (LE) in configuration 4. The second set of configurations simulates a large Gateway stack,

later in the spacecraft's assembly, in configuration 5. Orion arrives with a CMP (configuration 6), and then departs leaving the CMP in place (configuration 7).

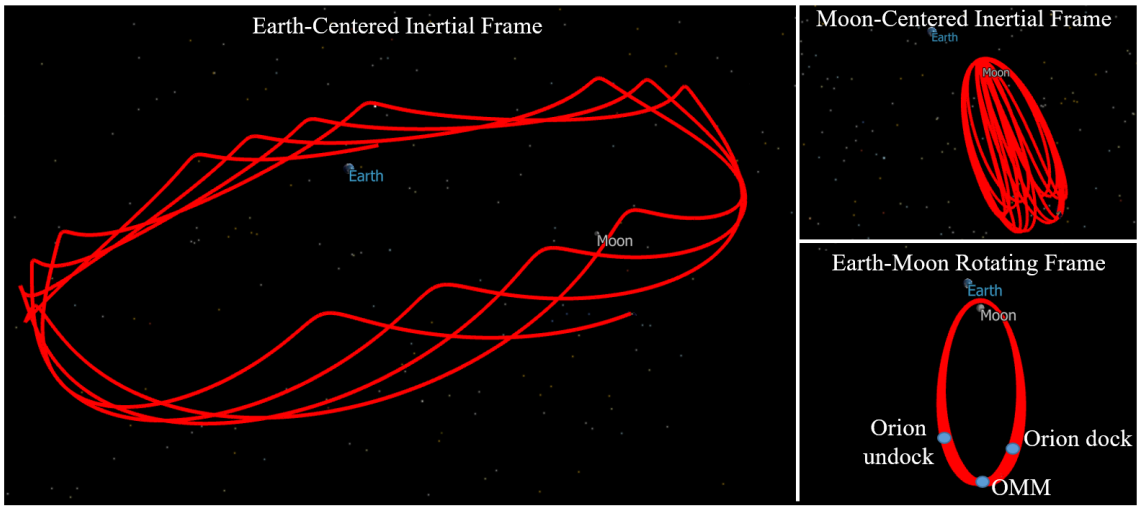

Figure 1. 9:2 Lunar synodic resonant NRHO in three reference frames

Table 1. Notional Gateway Configurations

Gateway Configuration	Description	Mass (t)
1	Small stack	7
2	Small stack + Orion + CMP	42
3	Small stack + CMP	15
4	Small stack + CMP + LE	29
5	Large stack	44
6	Large stack + Orion + CMP	80
7	Large stack + CMP	53
7b	Large stack + CMP: cross stack	53

Engine Models

The first component of the Gateway, the PPE is expected to carry two propulsion systems. The RCS system is assumed to include four thrusters powered by hydrazine propellant, each providing a 20 N thrust with a mass flow rate of 0.01 kg/s. The RCS thrusters are assumed to be located on the vertices and orthogonal to the faces of the PPE with an I_{sp} of 200s. The SEP system is powered by xenon propellant, and for orbit maintenance, two thrusters are assumed to be available for a given maneuver, each with a thrust of 1.132 N and a mass flow rate of 2.2931E-5 kg/s.

Crewed Spacecraft Constraints

The Gateway is planned as a crew-tended destination. The Orion spacecraft will transport crew from Earth to the NRHO, docking at the station and staying for up to 30 days. Orion thermal constraints require the spacecraft to be oriented within ±20° of a tail-to-Sun attitude, with a maximum 3-hour excursion from the nominal attitude. For this reason, slew rates and burn durations are important when crew is present on the Gateway. It is assumed in this study that during crew visits, slews to maneuver attitude and the OMMs themselves are performed using RCS thrusters. During uncrewed periods, reaction wheels or CMGs are used for slews, and the more efficient SEP thrusters perform OMMs.

Error Assumptions

While traveling along the reference NRHO, errors and perturbations affect the motion of the spacecraft. These effects vary as the Gateway stack is constructed and as crews arrive and depart the Gateway. The simulations consider errors and perturbations using two methods. In the orbit maintenance and attitude analyses, the errors are applied in a Monte Carlo process. In the OD analysis, a linear covariance analysis is

performed. In each of the analyses, the same sets of errors are considered. The baseline set of randomized errors and perturbations are listed in Table 2.

Table 2. Error models for crewed and uncrewed spacecraft configurations

Error/Perturbation	*Phases*	*3-sigma value*	*Frequency*	*Direction*
Insertion error	Initial	20 km, 20 cm/s	At insertion	Random
Navigation error	All	10 km, 10 cm/s	At each OMM	Random
SRP error	All	30% area, 15% C_R	Area: each rev C_R: each case	Random
Attitude error	All	1 deg	After every slew	Random
Desaturation perturbation	Uncrewed	3 cm/s	1 per rev	Random
OMM execution error: SEP	Uncrewed	1.42 mm/s + 1.5%	At each SEP OMM	Random
Docking perturbation	Dock + undock	0.1 m/s	At dock + undock	{-1, 0, 0} body-fixed
Desaturation perturbation	Crewed	3 cm/s	1 per 140 min	Random
OMM execution error: RCS	Crewed	1%	At each RCS OMM	Random
RCS slew perturbation	Crewed	5.649e-2 kgm/s	Pre and post-OMM	Random
CO_2 puff perturbation	Crewed	67.62 kgm/s	10 min	{-0.5, -0.866, 0.0} body-fixed
Wastewater dump perturbation	Crewed	153.61 kgm/s	3 hours	{-0.5, 0.0, -0.866} body-fixed

In the Monte Carlo analyses, Carbon Dioxide (CO_2) puff perturbations and wastewater dump perturbations (together referred to as "venting") along with the Reaction Control System (RCS) slew perturbations, are all divided by the current mass of the Gateway to apply a velocity perturbation; the values are consistent with Orion analysis.[10] Although RCS slews are planned to be executed by the PPE rather than Orion, error values from Orion analysis are employed in the current analysis since PPE estimates are not yet available. The venting and docking perturbations are applied in a constant direction in the body frame. Insertion errors, navigation errors, and slew and desaturation perturbations are applied in random directions. The venting, slew, and docking perturbations are applied as fixed-magnitude errors in the Monte Carlo analyses and as 3σ errors in the OD covariance analysis.

Modeling Considerations

The current analysis is performed in a high-fidelity ephemeris force model using the FreeFlyer COTS software package and the MONTE GOTS orbit determination program. The positions of the Earth, Sun, and Moon are taken from the NAIF de430 planetary ephemeris. The Sun and Earth are modeled as point masses, and the Moon's effects are computed with the Grail gravity model truncated to degree and order 8.

FINITE BURN STATIONKEEPING

With a proposed 15-year mission, the Gateway is planned to execute long-term operations in its primary orbit. While a spacecraft in an NRHO exhibits nearly stable behavior, if uncontrolled, it will depart the vicinity of the Moon after several months without orbit maintenance. An effective stationkeeping strategy is thus required. Previous studies[2-4] have identified low cost, reliable NRHO stationkeeping methods that employ impulsive burns. In the current investigation, an *x*-axis crossing control algorithm is extended to allow the maneuvers to take place using finite burns, effective with either the SEP or RCS thrusters on the PPE. The annual costs of stationkeeping for an uncrewed Gateway are computed using Monte Carlo analysis. Effects of docking perturbations are explored, as are the costs and risks of skipped maneuvers.

X-axis Crossing Control

As previously described,[2-4] an *x*-axis crossing control algorithm applies a maneuver at a specified point along a trajectory to target a given set of parameters further downstream. Such algorithms have been, and are currently, successfully used to maintain various spacecraft in halo orbits; examples include ARTEMIS[11] in the Earth-Moon system and WIND[12] currently in a Sun-Earth halo orbit. For the NRHO, the algorithm is

adapted to account for the shorter orbital period, the increased stability characteristics, and closer approaches to the Moon as compared to previously flown halo orbits.

The current study makes use of a long-horizon reference orbit in the targeting process. A maneuver adjusts the spacecraft trajectory to target component(s) of the reference orbit along a receding horizon. The placement of the maneuver and target, the components targeted, and the length of the targeting horizon all affect the cost and robustness of the stationkeeping algorithm. For the L_2 NRHO, to avoid introducing errors at the sensitive region near perilune, which can lead to algorithm divergence, maneuvers are placed at or near apolune. The target is placed at the *x*-*z* plane crossing near perilune, or at the nearby perilune itself, as this target location is observed to lead to lower orbit maintenance costs. A single component of the reference trajectory is selected as the target: the *x* component of rotating velocity in the Earth-Moon rotating frame, v_x. Targeting the single component results in a trajectory that remains near the reference for low cost. A longer targeting horizon tends to lead to lower maneuver costs. However, especially in the presence of large perturbations, the targeter may converge less reliably as the horizon increases. In the current study, a horizon of 6.5 revolutions is selected. If the targeter fails to converge, the horizon is successively reduced by 2 revolutions until convergence is achieved. In summary, the algorithm in the current investigation executes a maneuver at apolune to target the *x* component of rotating velocity, v_x, in the Earth-Moon rotating frame at the *x*-*z* plane crossing near perilune 6.5 revolutions downstream. Further details on the *x*-axis crossing control algorithm as implemented with impulsive maneuvers appear in Guzzetti et al.[3]

To better approximate the SEP and RCS thrusters and to effectively estimate the burn durations and propellant costs, the algorithm is adjusted to simulate finite burns instead of impulsive maneuvers. It is effective but unnecessary to employ finite burns in the targeting process itself—doing so increases computation time without reducing orbit maintenance cost. Even for long SEP burns, which can last multiple hours, the ideal rocket equation adequately converts between Δv and burn duration for OMMs performed near apolune in the NRHO. Therefore, the differential corrector estimates an impulsive burn magnitude and direction, which is then executed as a finite maneuver. The targeting process proceeds as follows:

1. Propagate the spacecraft to apolune.
2. Employ a differential corrector to target the three components of an impulsive maneuver that achieves a value $v_x = v_{xref}$ at perilune 6.5 revolutions downstream, yielding Δv magnitude and direction. If the targeter fails to converge, reduce the horizon.
3. Using the ideal rocket equation, compute the equivalent finite burn duration from the Δv magnitude for a given stack configuration.
4. If the maneuver magnitude is larger than a specified minimum, execute the computed finite burn.
5. Propagate the spacecraft a single revolution forward and repeat, applying errors as described in Table 2.

This algorithm effectively controls a spacecraft in the 9:2 LSR L_2 NRHO for both quiet, uninhabited spacecraft and noisy, crewed spacecraft configurations.

Uncrewed Operations

Consider a spacecraft orbiting in an NRHO for a year without crew, with attitude control performed by a passive ACS (reaction wheels or CMGs) and orbit maintenance performed by SEP xenon thrusters. In the 9:2 LSR NRHO, a year is equivalent to about 56 revolutions around the Moon. Such an uninhabited spacecraft is likely to demonstrate relatively quiet behavior, subject to insertion or delivery errors upon arrival, navigation knowledge errors, maneuver execution errors, SRP errors, and desaturation errors once per revolution. Without orbit maintenance, such errors as defined in Table 2 cause the spacecraft to depart the NRHO in 10-14 revolutions, or about 65-90 days. By applying *x*-axis crossing control, the spacecraft is maintained in the orbit for extended durations.

Assume a spacecraft is inserted into the 9:2 LSR NRHO at apolune. For an uncrewed 15,000 kg stack (configuration 3 in Table 1), the OMM magnitude history for 56 revolutions in the NRHO for a single representative run appears in appears in Figure 2a. Note that the magnitude of each burn is small, generally remaining below 10 cm/s. For this uncrewed scenario, it is assumed that the xenon SEP thrusters execute the maneuvers. Durations of the executed finite burns for 10 representative Monte Carlo trials appear in Figure 3a. Maneuver durations generally remain under half an hour.

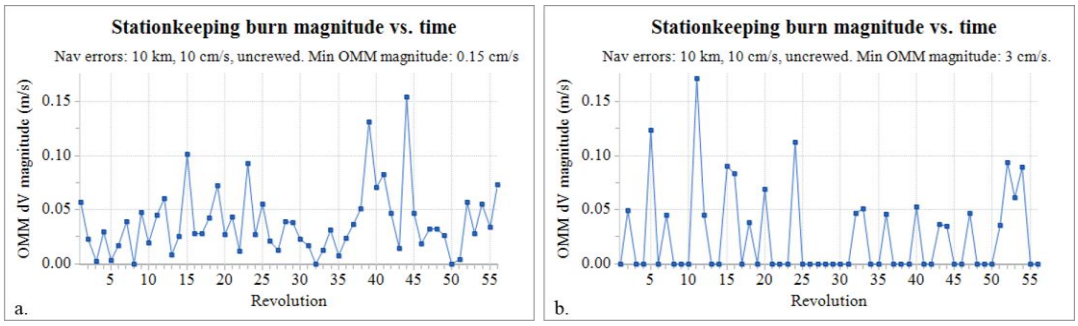

Figure 2. OMM Δ*v* magnitudes for 56 revolutions in the NRHO for two single representative runs. Minimum OMM magnitude = 0.15 cm/s (a) and 3 cm/s (b).

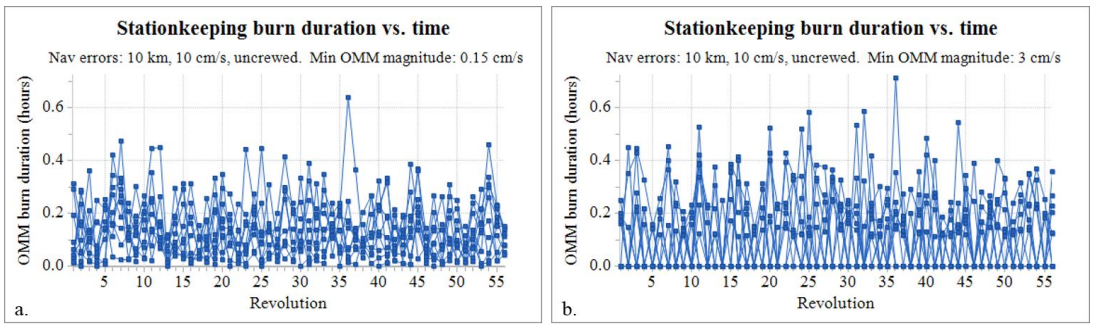

Figure 3. OMM durations for 56 revolutions in the NRHO for 10 Monte Carlo trials for each of two cases. Minimum OMM magnitude = 0.15 cm/s (a) and 3 cm/s (b).

The Monte Carlo trials in Figures 2a and 3a are computed with a minimum OMM magnitude threshold set to 0.15 cm/s, a representative operational minimum for the thrusters on the PPE. That is, a given OMM is executed only if its targeted magnitude is greater than the threshold. With the minimum OMM threshold set to 0.15 cm/s, only 3 computed OMMs fall below the threshold, and the spacecraft slews away from SPEA to the OMM attitude and back 53 times during the year of uncrewed operations. The number of OMMs, and the corresponding number of required slews and time away from SPEA, are reduced by raising the minimum OMM threshold to 3 cm/s. The Δ*v* magnitude history for a single representative case appears in Figure 2b. With a threshold of 3 cm/s, 35 maneuvers are skipped in the case corresponding to Figure 2b, reducing by more than half the number of required slews without an increase in total cost. The burn durations for 10 representative Monte Carlo trials appear in Figure 3b. While individual burn durations can be larger when the minimum OMM threshold is increased, no individual maneuver is longer than 45 minutes, and very short maneuvers are avoided completely. It is apparent from Figure 3 that the number of skipped maneuvers with duration = 0 is significantly higher with the higher threshold. When a longer Monte Carlo run is performed including 100 trials per case, the resulting costs appear in Table 3. The total annual orbit maintenance cost is slightly reduced by raising the minimum maneuver threshold, with a mean annual cost of 1.95 m/s (or 1.2 kg xenon) with a 0.15 cm/s OMM threshold and a mean annual cost of 1.84 m/s (or 1.1 kg xenon) with a 3 cm/s OMM threshold. More significantly, raising the threshold also increases the number of skipped maneuvers. With the small OMM threshold, the 100 Monte Carlo trials average 1.6 skipped maneuvers per trial. The larger OMM threshold, on the other hand, yields an average of 25.7 skipped maneuvers per trial, with a minimum of 17 skipped burns and a maximum of 39 skipped OMMs. That is, on average, an OMM is only required about every other revolution when the OMM threshold is set to 3 cm/s. Not surprisingly, the mean duration of nonzero burns is about double (0.23 hours) with the larger OMM threshold as compared to 0.13 hours with the smaller threshold. The OM algorithm reliability is 100% in both cases, that is, all Monte Carlo trials finish successfully without failing to target the reference NRHO at any point. However, it is observed that raising the threshold above 3 cm/s can increase cost and affect algorithm reliability for higher navigation errors or for crewed spacecraft configurations. In summary, carefully setting the OMM threshold can reduce the number of required OMMs (and associated slews) by nearly half

without negatively affecting either OM cost or algorithm reliability. The mean annual cost for uncrewed orbit maintenance using SEP thrusters is less than 2 m/s annually, or just over a kilogram of xenon propellant, and the maximum burn duration is less than an hour, when navigation and spacecraft errors are considered as specified in Table 2.

The uncrewed Monte Carlo analysis is repeated with a minimum maneuver threshold of 3 cm/s for additional configurations. The results appear in Table 3. The annual Δv cost does not vary significantly with stack mass. While desaturation have a larger effect on smaller stacks, they occur only once per revolution for uncrewed configurations, and the effects are small. The annual xenon propellant mass use scales with the stack mass, as depicted in Figure 4.

Table 3. Annual OM costs for uncrewed spacecraft with varying OMM thresholds and masses

Thresh-old	Con-fig	Mass	Annual Δv (m/s)			Annual Xenon (kg)			OMM durations (hrs)			skipped burns		
		(t)	min	mean	max	min	mean	max	min	mean	max	min	mean	max
.15 cm/s	3	15	1.56	1.95	2.61	1.0	1.2	1.6	0.01	0.13	0.76	0	1.6	5
3 cm/s	3	15	1.17	1.84	2.45	0.7	1.1	1.5	0.11	0.23	0.81	17	25.7	39
3 cm/s	1	7	1.31	1.91	2.47	0.4	0.6	0.7	0.05	0.11	0.42	18	25.5	35
3 cm/s	5	44	0.94	1.81	2.37	1.7	3.2	4.2	0.32	0.65	2.11	17	26.0	37
3 cm/s	7	53	1.35	1.86	2.31	2.9	4.0	5.0	0.39	0.80	2.94	20	25.7	35

The OMM directions computed by the differential corrector are not random. For the 10-trial Monte Carlo run represented in Figure 3b, each Δv is normalized and the Δv_y and Δv_z components are plotted versus Δv_x in the Earth-Moon rotating frame in Figure 5. The Δv_y vs. Δv_x direction for each OMM appears as a solid blue line, and Δv_z vs. Δv_x for each OMM appears as a solid red line. Note that the directions are all generally aligned in the Earth-Moon rotating frame. Similar analysis during and after the ARTEMIS mission demonstrated that the optimal stationkeeping maneuvers computed for the two ARTEMIS spacecraft generally aligned with the eigenvector of the stable mode corresponding to the unstable halos in which the spacecraft flew.[10] Similarly, WIND stationkeeping takes advantage of this knowledge; OMMs for the WIND spacecraft are designed in the stable mode direction corresponding to its Sun-Earth halo orbit.[11] The NRHO is nearly stable, and its stable eigenvector definition is thus not well defined. However, the stable eigenvector components (y vs. x and z vs. x) for an unstable Earth-Moon halo orbit (with r_p = 47,985 km) are computed at apolune in the CR3BP and are also plotted in dark dotted lines over the OMM components in Figure 5. The unstable halo directions are closely aligned to the OMM directions for the 9:2 LSR NRHO. It is noted in Davis et al.[4] that the stable eigenvector direction for a given halo orbit approximates the targeted OMM direction for L_2 halos with r_p values ranging from about 35,000 km to 51,000 km (corresponding to a very flat, nearly Lyapunov-like halo). As the halos approach the moon and become more stable, the r_p values decrease, and the eigenvector directions become less well defined, ceasing to be an effective approximation for the OMM directions. Note that, although the OMM directions are consistent in the Earth-Moon rotating frame, the direction of the OMM relative to the Sun rotates through 360º during each month.

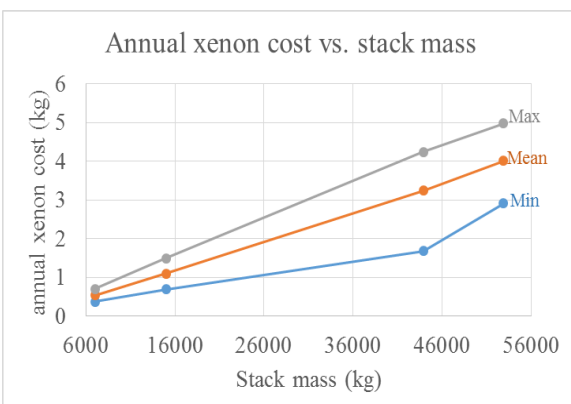

Figure 4. Annual Xenon propellant use as a function of stack mass.

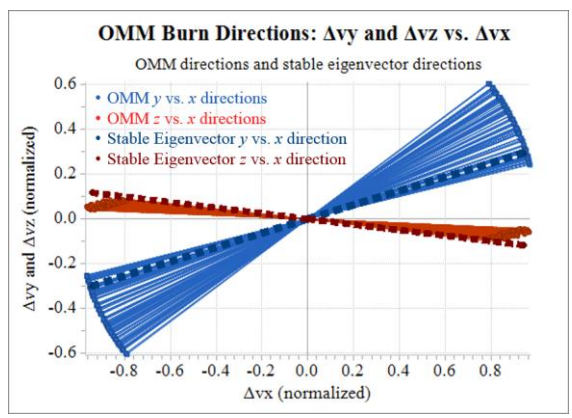

Figure 5. Normalized OMM burn directions in the Earth-Moon rotating frame: *y* vs. *x* (blue) and *z* vs. *x* (red) for a year of OMMs.

So far, the analyses have assumed OD knowledge errors of 10 km in position and 10 cm/s in velocity (3σ) and insertion delivery errors, applied at apolune, of double the OD knowledge errors. The orbit maintenance costs for both crewed and uncrewed spacecraft scale with the OD errors. In Figure 6, the minimum, mean, and maximum annual stationkeeping costs for an uncrewed spacecraft appear as a function on OD knowledge errors. With perfect navigation (but still considering SRP, desaturation, and OMM execution errors as specified in Table 2), the OM costs are small, with a mean of 0.67 m/s per year. As navigation errors increase, the costs also increase. The mean annual costs increase approximately linearly to a value of about 20 m/s for navigation errors of 100 km and 100 cm/s (3σ), but the maximum costs increase at a steeper rate and can have large excursions. Thus, it is important to achieve accurate orbit determination to ensure low stationkeeping costs.

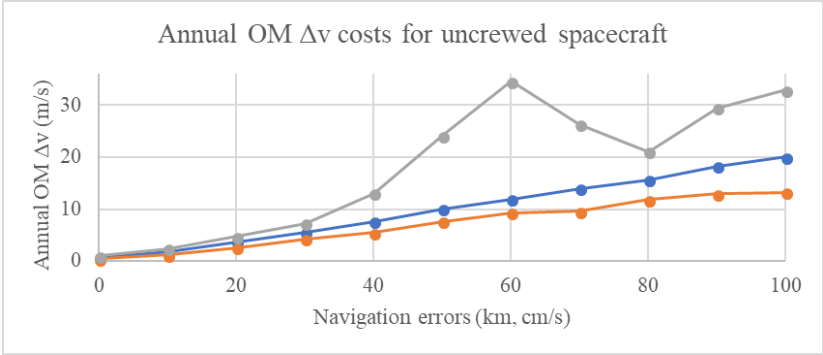

Figure 6. Min, mean, and max OM costs for uncrewed spacecraft as a function of OD accuracy

Orion Docking and Crewed Operations: Short Stay

The Gateway is envisioned as a crew-tended depot with periodic visits from the Orion spacecraft. Orbit maintenance is analyzed for two docking scenarios. The first considers a short Orion stay in a small stack, corresponding to configurations 1, 2, and 3 in Table 1. In this scenario, the PPE performs uncrewed operations for several revolutions in the 9:2 LSR NRHO, with OMMs executed using the xenon-powered SEP engines. The Gateway is then joined by Orion, carrying a crew and a comanifested payload. Docking occurs about 1.3 days after perilune. At docking, a perturbation representing plume impingement and physical docking forces is applied. At apolune, an OMM mitigates the docking perturbation. Orion vents periodically while it is docked for one full revolution with one perilune pass. A second OMM is performed at apolune about 1.75 days prior to undocking. Approximate dock, OMM, and undock locations appear in Figure 1. Since excursions from Orion's tail-to-Sun attitude must last less than 3 hours, it is assumed that slews to and from OMM attitude are performed using RCS thrusters and thus impart a Δv on the Gateway. The OMMs themselves are also executed using the hydrazine-powered RCS thrusters to limit time away from Orion tail-to-Sun attitude. During the crew's residence on the Gateway, CO_2 puffs occur every 10 minutes on average, and wastewater dumps are executed every 3 hours. These venting perturbations impart both Δv and angular momentum on the Gateway; wheel/CMG desaturations are assumed to occur just once per revolution during uncrewed operations but are applied every 140 minutes during crewed operations. At Orion departure, an undocking perturbation is applied to the Gateway, after which the Gateway stack remains in uncrewed operations for the rest of the year, with OMMs again provided by SEP thrusters.

To explore the xenon and hydrazine propellant costs for a year of Gateway operations including a short Orion stay, a Monte Carlo analysis is performed, assuming error levels as specified in Table 2. Representative sets of OMMs appear in Figure 7. The maneuver Δv magnitudes appear in Figure 7a. The blue markers represent uncrewed revolutions with OMMs executed using the SEP thrusters and xenon propellant. The red markers correspond to crewed revolutions with OMMs performed using the RCS thrusters and hydrazine propellant. Note the larger post-dock and post-undock OMMs; these maneuvers serve to clean up after the dock and undock perturbations on the Gateway. The second crewed OMM in red is also relatively large, accounting for crewed perturbations including venting and frequent desaturations. The maneuver durations appear in Figure 7b. The OMMs in red are executed with the RCS thrusters and thus are shorter in duration despite their larger magnitudes. Note that the post-undock SEP OMM durations are generally longer than the pre-dock SEP OMMs; this occurs because Orion has delivered a comanifested payload to the Gateway; the stack is more massive after Orion's departure.

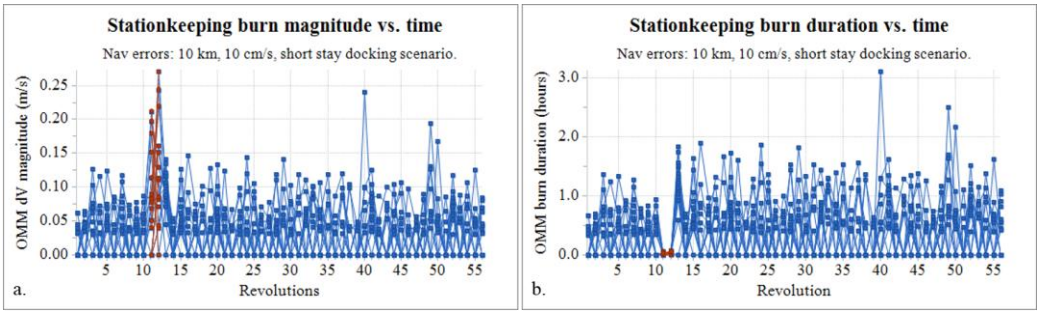

Figure 7. OMM maneuver magnitudes and durations for a short-stay docking scenario

For the short-stay docking simulation, 500 Monte Carlo trials are run for 56 revolutions each for a series of cases to explore the effects of docking perturbations. The associated costs, Δv and mass of hydrazine and xenon propellant appear in Table 4. Row 1 represents the nominal setup as specified in Table 2. With a docking and undocking perturbation of 10 cm/s each, the mean total xenon cost, 1.88 m/s or 1.1 kg, is slightly higher than the annual uncrewed cost appearing in Table 3 due to cleanup from the undocking perturbation. The mean total hydrazine cost is only 0.49 m/s but requires nearly 10 kg of hydrazine to execute. Rows 2-4 explore varying docking perturbations; large docking perturbations significantly affect hydrazine cost, with a mean mass of 27.6 kg of hydrazine required to maintain the crew during Orion's short stay if the docking perturbation reaches 1 m/s.

Table 4. Hydrazine and xenon OM propellant costs for one year with a short-stay Orion visit

	hydrazine Δv (m/s)			hydrazine mass (kg)			xenon Δv (m/s)			xenon mass (kg)		
dock (cm/s)	min	mean	max	min	mean	max	min	mean	max	min	mean	max
10	0.10	0.44	0.68	4.1	9.8	16.2	1.18	1.88	2.49	0.7	1.0	1.4
2	0.05	0.35	0.67	2.2	8.2	15.3	1.11	1.81	2.44	0.6	1.0	1.3
50	0.51	0.84	1.11	12.1	17.4	22.8	1.72	2.31	3.04	0.8	1.3	1.7
100	1.04	1.34	1.65	21.3	27.6	33.8	2.23	2.91	3.70	1.3	1.7	2.1

Because docking and venting perturbations occur in a body-fixed frame, and because the Gateway is oriented in an Orion tail-to-Sun attitude during crewed operations, the location of the Sun relative to the NRHO at dock and during crewed operations affects the OMM cost during crewed operations. Since the NRHO is in a 9:2 lunar synodic resonance designed to avoid eclipses by the Earth's shadow, there are effectively 9 different possible orientations of the Gateway relative to the Sun at any given OMM location. To confirm that the stationkeeping cost is affected by the solar orientation, the docking is placed at 27 different revolutions, one at a time, along the NRHO. For each docking location, 100 Monte Carlo trials are run for a one year simulation with a short-stay Orion visit, and the mean hydrazine costs are recorded. The runs are grouped in sets of 9 according to docking location, and the mean Δv is plotted vs. solar orientation in Figure 8. The 0.49 m/s hydrazine cost reported in Table 4 represents a docking at rev 10, corresponding to solar orientation 1. However, depending on the solar orientation, the hydrazine cost can be as low as 0.24 m/s or as high as 0.79 m/s for maintaining the Gateway during the short stay, representing a variation of about 11 kg between the minimum and maximum.

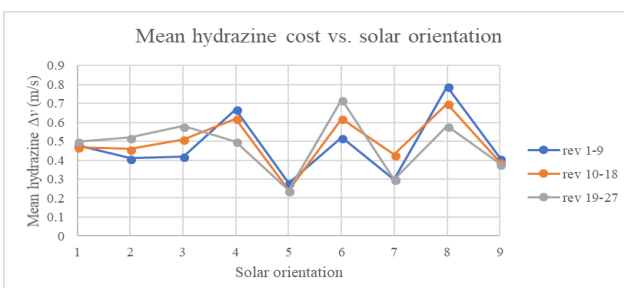

Figure 8. Mean OM hydrazine cost for a short stay as a function of solar orientation

Orion Docking and Crewed Operations: Long Stay

Consider a second docking scenario occurring later in the Gateway's lifetime. A larger stack corresponding to configuration 5 in Table 1 is joined by Orion carrying a comanifested payload. This time, Orion stays for 30 days, or 4 full revolutions in the NRHO (configuration 6), before undocking and leaving the payload behind (configuration 7). OMM Δv magnitudes and burn durations based on 30 Monte Carlo trials appear in Figure 9 for an Orion long stay scenario with errors applied according to Table 2. As in the short stay scenario, the blue markers represent uncrewed OMMs executed by the SEP thrusters and red markers signify crewed OMMs performed by the RCS thrusters. As expected, many zero-magnitude revolutions are visible during the uncrewed revolutions, but it is notable that the additional errors applied during crewed revs lead to an OMM being executed at every apolune during crewed operations. The burn magnitudes in Figure 9a indicate the larger OMMs required to maintain the spacecraft in the NRHO when the Gateway is inhabited. Note that the large burn at revolution 15 is attributable to the solar orientation; regardless of which revolution contains the docking itself, the solar orientation at revolution 15 leads to a large OMM at that apolune. However, the solar orientation at docking can affect the total cost.

Because the OMMs during crewed operations are executed using the RCS thrusters to reduce the time Orion is away from a tail-to-Sun attitude, the burn durations (Figure 9b) during crewed operations (in red) are low. The post-undock SEP OMMs in blue have similar Δv magnitudes but longer durations as compared to the pre-dock SEP OMMs because the Gateway stack is more massive after the comanifested payload is delivered. Note the large post-undock maneuver performed by the Xenon thrusters (in blue) visible in Figure 9b; this maneuver cleans up the undock perturbation as well as errors in the Gateway orbit accumulated during the crewed revolutions. Note also the duration of this larger maneuver, of up to 1 hour. The magnitude of this burn is considerably smaller (as apparent in Figure 9a) than some of the crewed OMMs in red. Thus, if the SEP thrusters are employed to execute large OMMs during crewed operations, the Orion tail-to-Sun attitude constraint will risk violation.

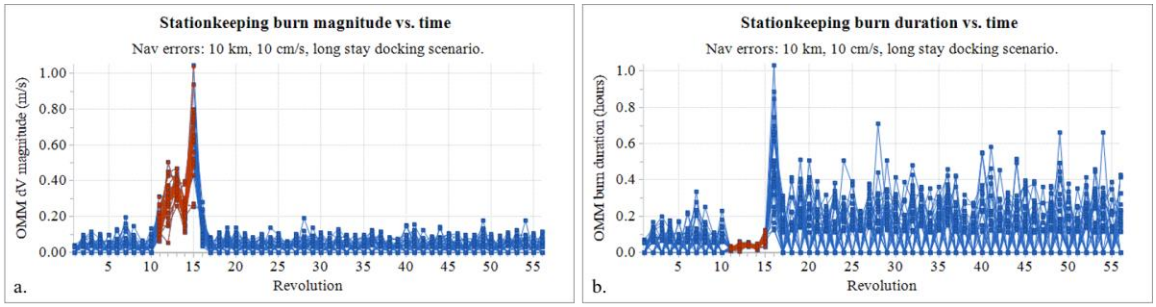

Figure 9. OMM burn magnitudes and durations for an Orion long stay docking scenario: 10 cm/s docking perturbations, 30 Monte Carlo trials

During crewed operations, OMM Δv costs are higher due to the venting and associated frequent desaturations. To explore the effects of crewed perturbations on OM costs, a series of Monte Carlo analyses are run; results appear in Table 5. Each row in the table represents 500 Monte Carlo trials. Row 1 represents the nominal case with errors applied as specified in Table 2. In this case, CO_2 puffs and wastewater dumps are active, and a desaturation with a 1 cm/s error (3σ) is applied every 140 minutes. The longer crew stay does not significantly affect the xenon Δv costs as compared to the short stay results in the first row of Table 4, though the xenon mass expenditure is considerably higher since the stack mass is larger. The hydrazine Δv costs are higher for the long stay scenario, since five (rather than two) OMMs are executed using hydrazine propellant. Rows 2 and 3 of Table 5 explore the effects of the desaturations themselves. With only one desaturation per rev during uncrewed ops, their error level has negligible effect on the xenon cost. During crewed operations, desaturations are assumed to occur every 140 minutes, and increasing the magnitude of the associated errors significantly increases the maximum hydrazine costs, though the mean values do not significantly vary with changing desaturation errors. If CO_2 puffs are eliminated, the hydrazine costs are reduced by over half, as seen in row 4 of Table 5. If wastewater dumps are also removed from the simulation (row 5), the hydrazine propellant mass is reduced to just a third of the value in row 1.

Table 5. Hydrazine and xenon OM propellant costs for one year with a long-stay Orion visit

	hydrazine ΔV (m/s)			hydrazine mass (kg)			xenon ΔV (m/s)			xenon mass (kg)		
Desaturation (cm/s) /venting	min	mean	max	min	mean	max	min	mean	max	min	mean	max
1/WW+CO_2	0.28	0.77	1.93	11.0	30.8	76.9	1.20	1.80	7.88	2.5	3.8	16.8
0.1/ WW+ CO_2	0.36	0.76	1.06	14.4	30.2	42.3	1.20	1.80	2.44	2.3	3.8	5.4
2/ WW+ CO_2	0.13	0.92	5.79	5.1	36.6	230.4	1.12	1.79	2.49	2.3	3.7	5.2
1/WW only	0.00	0.34	0.86	0.0	13.5	34.1	1.14	1.77	2.54	2.4	3.7	5.3
1/no venting	0.04	0.24	0.50	1.7	9.5	20.1	1.18	1.78	2.47	2.5	3.7	5.2

It is interesting to note that the mean hydrazine Δ*v* costs associated with a *long* stay in a *small* stack (configurations 1-3 from Table 1) are more than double the cost associated with a long stay in a large stack (configurations 5-7 from Table 1). This occurs because Orion venting has a larger perturbing effect on the stack of smaller mass. However, since the thrusters have a similarly increased influence on the smaller stack, the mean hydrazine propellant mass expended during a long stay is nearly the same for both the small and large Gateway stack.

In the current analysis, OMMs while Orion is docked are executed using RCS thrusters to minimize time away from Orion tail-to-Sun attitude, as previously noted. It is also possible to split a long SEP OMM into two equal pieces, for example by executing half of the OMM at 12 hours prior to apolune passage, and the second half of the OMM 9 hours after apolune passage. Assuming each excursion from the desired attitude is 3 hours long, this scenario gives the Gateway 18 hours between the two burn sequences. Splitting the maneuver in this manner does not adversely affect algorithm reliability or total OMM Δ*v* cost. However, it doubles the number of slews required to execute the total OMM set. Since the slews during crew visits are assumed to be performed using RCS thrusters, hydrazine savings achieved by splitting maneuvers have not been observed.

Missed Orbit Maintenance Maneuvers

During its lifetime, the Gateway may experience missed maneuvers, due either to operational preferences or to mission anomalies. The effects on the Gateway orbit differ depending on whether the skipped maneuvers are during crewed or uncrewed operations. Recovery costs depend on the solar orientation during docking perturbations and crewed revs. Two scenarios are explored: purposely skipped maneuvers to allow undisturbed refueling during uncrewed operations, and missed OMMs during crewed operations when noisy perturbations act on the Gateway.

Consider a scenario in which a logistics element (LE) is delivered to the Gateway autonomously, carrying xenon propellant to replenish the Gateway's reserves. The resulting stack is assembled in configuration 4 from Table 1. A post-dock OMM is executed to mitigate a 10 cm/s (3σ) docking perturbation, but no undocking is performed; the LE is assumed to remain fixed to the Gateway after refueling. During the refueling process, the Gateway is uninhabited, and no OMMs are performed during refueling. The effects on subsequent OMMs of skipping 1-3 OMMs after the post-dock cleanup burn to allow refueling to take place are explored in a Monte Carlo analysis. Sample OMM Δ*v* histories appear in Figure 10, and the mean annual xenon Δv costs are summarized in Table 6. Skipping a single OMM, resulting in a 13 day quiet period for refueling, has a negligible effect on the OMM when stationkeeping resumes, as depicted in Figure 10a, and the annual cost is unchanged in a 100-trial Monte Carlo simulation. The analysis is also run considering docking at 18 different revolutions to assess the effects of the Sun's orientation on the cost, and the mean annual Δv costs vary by 0.12 m/s with changing solar orientation at docking. If a second OMM is skipped, the quiet period is extended to about 20 days, but a noticeable increase in the magnitude of the recovery maneuver is visible in Figure 10b. The annual Δ*v* cost is increased by a small value, 0.08 m/s. After skipping a third maneuver for a 26 day quiet period, the recovery OMM can be large, with magnitudes over 0.5 m/s, as in Figure 10c. Although the recovery maneuver may be relatively large, the mean annual OM cost is only increased by 0.2 m/s after 100 Monte Carlo trials as compared to a case with no skipped maneuvers.

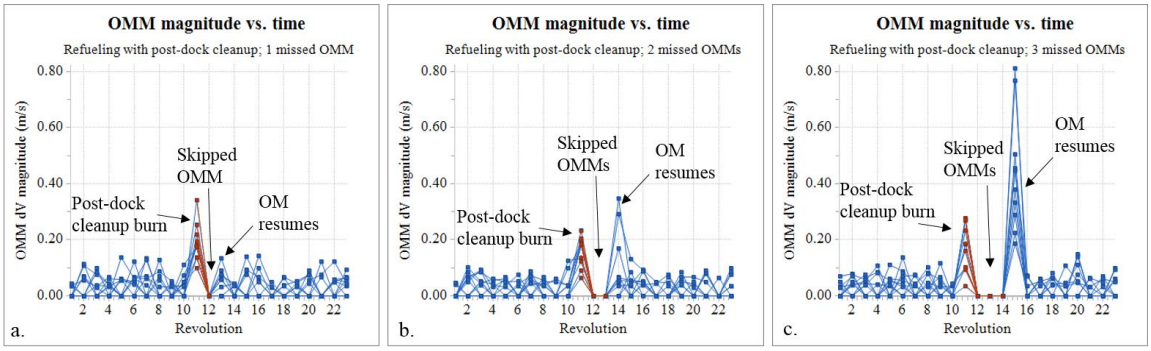

Figure 10. OMM Δ*v* magnitudes for an uncrewed refueling scenario. One (a), two (b), and three (c) skipped OMMs. Ten Monte Carlo trials per case.

Table 6. Xenon OM Δ*v* costs for an uncrewed refueling scenario

	Skipped OMMs for refueling (uncrewed scenario)			
100 Monte Carlo trials	0	1	2	3
Mean annual Δ*v*(m/s)	1.84	1.84	1.92	2.04

Not surprisingly, missing maneuvers while Orion is docked affects the OM process more significantly due to the larger perturbations associated with crewed operations, including docking, undocking, frequent desaturations, and venting. For operational reasons, it may appear desirable to avoid performing OMMs while Orion is docked. However, such a concept has significant effects on the orbit itself as well as on the xenon propellant budget. Two scenarios are explored as before: a short Orion stay in configuration 2 and a long Orion stay in configuration 6. The short stay includes one full revolution in the NRHO and two apolune passages; without OM during the crew visit, two OMMs are skipped in the short stay scenario, including the post-dock cleanup maneuver. With errors considered as specified in Table 2, a sample OMM magnitude history appears in Figure 11a for 25 Monte Carlo trials. Large post-undock cleanup maneuvers can exceed the combined cost of a year of nominal orbit maintenance. The annual costs based on 100 Monte Carlo trials appear in Table 7. The mean annual OM cost is about double the nominal cost, and individual cases are over 5 m/s.

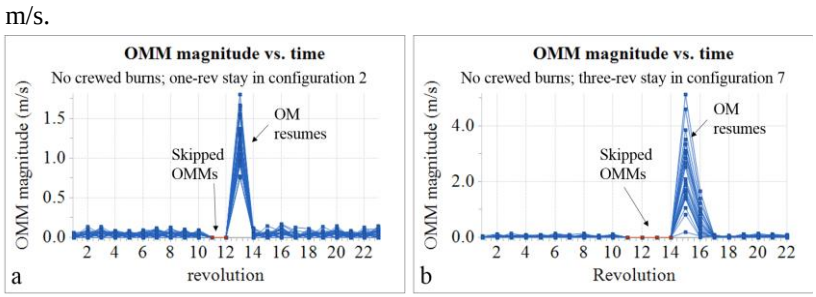

Figure 11. OMM Δ*v* magnitudes without crewed burns

For a long Orion stay, the effects of skipped maneuvers are still larger. A four-revolution stay incorporates five OMMs, including the post-dock cleanup maneuver. When all five OMMs are skipped, the targeter as implemented fails to converge on a solution in more than 15% of cases. Thus, costs are also considered for a three-revolution stay with four skipped OMMs. All 9 possible solar orientations at docking are considered, and the annual costs from the most and least favorable solar orientations for docking appear in Table 7 based on 100 Monte Carlo trials per case. A sample OMM history including 25 Monte Carlo trials appears in Figure 11b. Two large post-undock maneuvers are implemented after OM resumes, with individual OMMs as large as 4.5 m/s. The mean annual OM cost ranges from 2.8 to 5.5 m/s depending on docking location, with maximum costs up to nearly 12 m/s. In the worst-case docking orientation, the targeter fails to converge after the post-undock cleanup maneuver in 5% of cases.

While skipping OMMs when Orion is docked does not appear to risk orbit divergence for stays of up to three revolutions, depending on solar orientation at docking, the cost of post-undock cleanup maneuvers is large. The current analysis considers a total docking perturbation of 10 cm/s; larger docking forces increase

cost and risk. In addition, the post-undock NRHO has deviated from the reference, and the current analysis does not consider the cost of re-phasing the orbit for eclipse avoidance. For crewed visits longer than three full revolutions without OMMs, the OM algorithm as implemented in the current study is not robust.

Table 7. Annual xenon OM Δ*v* costs with no OM performed during Orion stay

100 Monte Carlo trials each	Min (m/s)	Mean (m/s)	Max (m/s)	failed cases
1 rev stay, configs 1-2-3	1.8	2.8	3.5	0
3 rev stay, configs 5-6-7 (best solar orientation)	1.4	2.8	6.0	0
3 rev stay, configs 5-6-7 (worst solar orientation)	1.7	5.5	11.7	5
4 rev stay, configs 5-6-7	1.3	6.5	13.4	16

ORBIT DETERMINATION

To assess OD uncertainties, a linear covariance analysis is conducted assuming DSN radiometric tracking measurements are available in varying amounts. Since the DSN stations are globally distributed (Madrid/Spain, Canberra/Australia, Goldstone/USA), near-continuous tracking is possible. While this is beneficial during crewed operations, it is desirable to understand the minimal tracking needs especially during uncrewed periods.

The DSN measurements used in this study are S-band, two-way Doppler and range. Simulated DSN ground station observations are constrained to be no longer than six-hours and to be above 10 deg elevation. Doppler measurements are assumed to be averaged over 60 seconds with 1 mm/s (1σ) random noise. Range measurements are simulated with 1 m (1σ) random noise and are accumulated over five-minute intervals. Key dynamical error sources affecting the OD knowledge include: attitude control reaction wheel desaturations, imperfect maneuver executions and venting due to crew related activities. Assumptions for the size and frequency of these error sources are derived from Table 2.

Figure 12 shows the OD performance assuming randomly selected DSN passes, three times per week. After a few DSN passes the a priori position and velocity uncertainties are reduced to steady-state levels. Due to thruster activities and significant non-linear dynamics around perilune (denoted by red vertical dashed lines), the errors increase dramatically during periods without DSN tracking. Figure 13 demonstrates the benefit of tailoring the DSN tracking request to ensure coverage spanning perilune and other dynamical events such as wheel desaturations (shown as light grey vertical dashed lines) and OMMs (shown as blue vertical dashed lines).

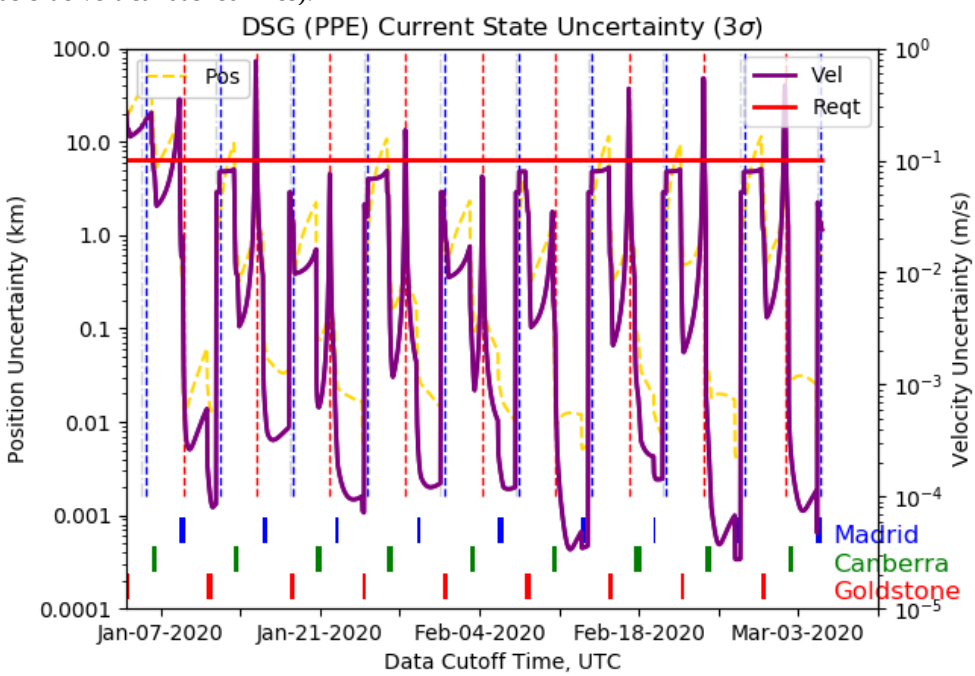

Figure 12. DSN Tracking: 3 Passes/Week (Randomly Selected)

During crewed operations the PPE wheel desaturation frequency increases markedly from once every orbit to once every 140 minutes. In addition, venting from the Orion crew element, as documented in D'Souza and Barton,[10] introduces OD errors as shown in Fig 14. With near-continuous tracking during crewed operations, velocity uncertainties from these error sources remain below the desired 10 cm/s (3σ) level.

Crew venting perturbations have the largest effect when the stack is least massive. The venting acceleration errors are directly proportional to the stack mass. For example, the CO_2 puff acceleration error in each axis for configuration 2 (42 t) is 4.4 x 10^{-7} m/s^2 (1σ). The acceleration uncertainties for the more massive stack of configuration 5 (80 t) is 2.3 x 10^{-7} m/s^2 (1σ).

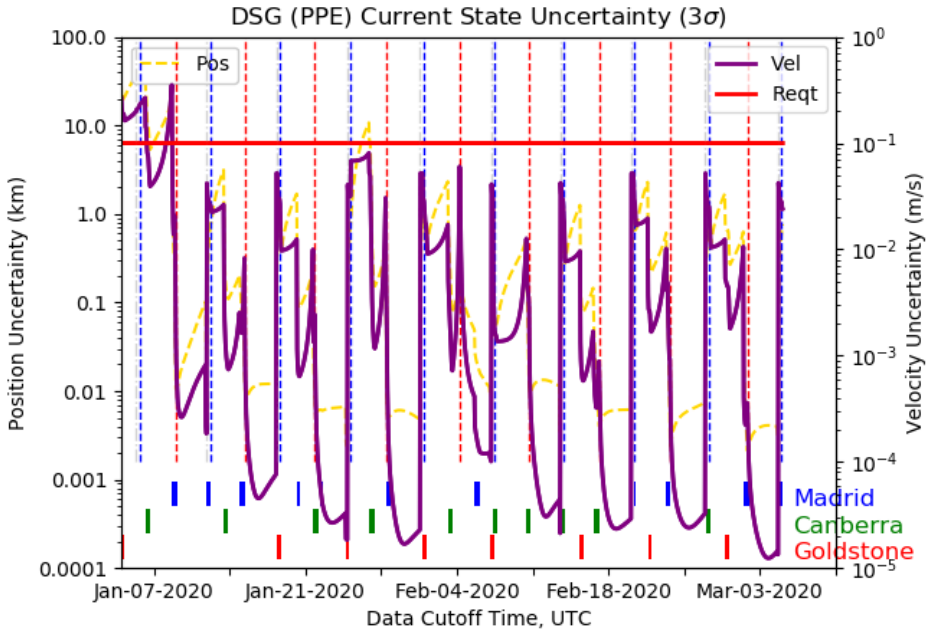

Figure 13. DSN Tracking: 3 Passes/Week (Tailored)

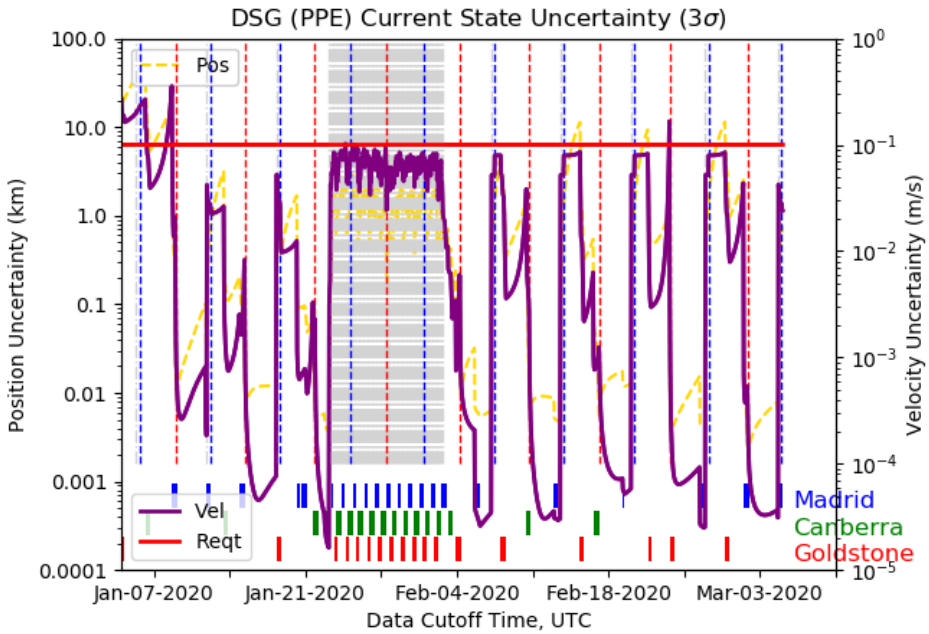

Figure 14. DSN Tracking: Continuous During Crewed Operations

Given the impact of wheel desaturation errors on the OD, additional sensitivity analysis results are shown in Fig 15. For uncrewed operations, three, six-hour DSN passes per week are adequate to maintain the OD knowledge to better than 10 cm/s (3σ) more than 90% of the time. When crew elements are included, the tracking requirements increase to nearly continuous.

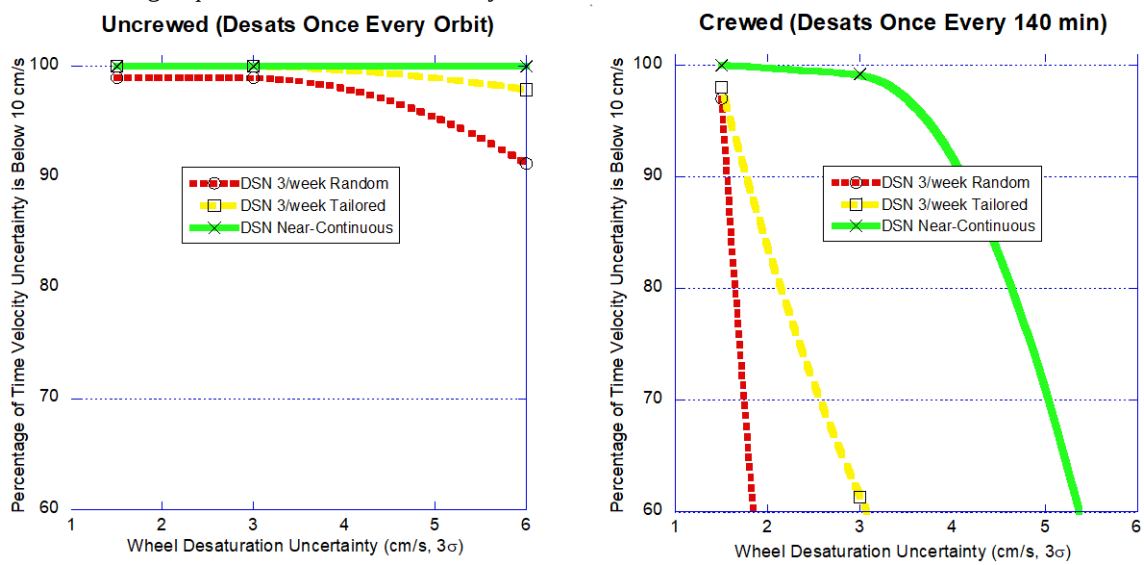

Figure 15. Sensitivity to Attitude Control Wheel Desaturation Uncertainties

ATTITUDE CONTROL IN NRHO

Spacecraft attitude operations are integrated into the Gateway analysis to target attitude profiles that minimize SRP torque, to assess CMG or reaction wheel sizing, and to estimate RCS propellant costs. The Gateway must maintain a nominal attitude that does not put unnecessary stress on its attitude control system. The Gateway must also be able to handle slews to different attitudes at a reasonable rate and without overloading the control system or wasting propellant. Previous studies have simulated the spacecraft in NRHO as a point mass in a three degree of freedom analysis.[1-4] The current investigation expands the spacecraft model to include a moment of inertia matrix and 3D surfaces in the spacecraft body frame to simulate SRP forces and torques on the spacecraft body.

Solar Pressure Equilibrium Attitude (SPEA)

The Gateway is nominally held in a SPEA to prevent angular momentum buildup in the wheelset from the uneven distribution of SRP forces. A flat plate model is employed to assess SRP forces, in which the panel size, location, and mass properties are defined for each component. A notional example composed of the PPE, a habitat, an airlock, and a logistics element appears in Figure 16. The Gateway is assembled from the component plates using the parallel axis theorem for combined Gateway mass properties. The solar arrays of the PPE and LE are pointed parallel to the body *z* axis, and they rotate about that axis to present their full face normal to sunlight direction. Solar panels and body panels have differing values of specular and diffuse coefficients of reflectivity. A differential corrector algorithm is employed to target an attitude with zero total torque from SRP. When Orion is docked axially, as in Figure 16a, the differential corrector converges to a SPEA at approximately 2º yaw from direct Orion tail-to-Sun. This is well within the requirement that Orion remain in a tail-to-Sun attitude ±20º. Conversely, if Orion is docked radially as in Figure 16b, the SPEA is 89º from Orion's tail-to-Sun direction. Thus, SPEA cannot be maintained while Orion is radially docked; a radial docking configuration results in significant deviations from SPEA and significant loading of the momentum management system.

Pixel-based SRP Force Modeling

The flat plate model is limited by not considering spacecraft self-shadowing. The complex shape of the Gateway, particularly while Orion is attached in a tail-to-sun orientation, results in plates of the flat plate model being partially or totally obscured from the Sun by other panels. In the flat plate model, the SRP force component is nevertheless included in the SRP force and moment summation. Additionally, as the

Gateway design evolves and different configurations and components are analyzed, it is beneficial to work directly with 3D models of components and assemblies to ensure the dimensions and associated parameters such as surface normals are derived directly from the models.

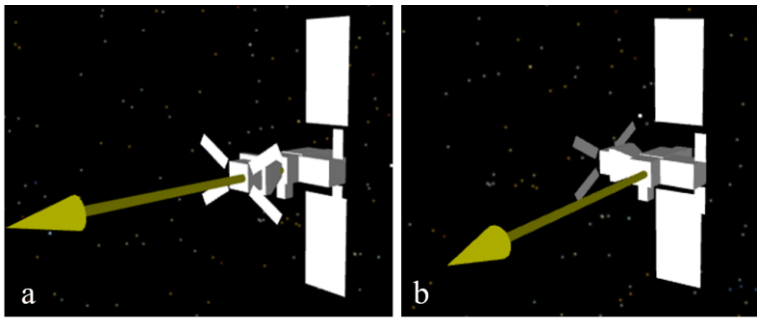

Figure 16. The flat plate model of the Gateway with Orion at SPEA. Orion is docked axially (a) and radially (b). Vector points to the Sun.

To this end, a pixel-based SRP force model is developed and tested against the flat plate model. The pixel-based model employs the same SRP force assumptions, but it builds the plates using a photon beam scan. The process is illustrated in Figure 17. A photon plane normal to the Sun-spacecraft vector is defined and located between the Gateway and the Sun as in Figure 17a. Vectors oriented along the SRP direction with tails on the plane are defined; the density of vectors from the photon plane depends on the desired resolution of the model. The length to first contact from the photon plane to the 3D model is computed for each vector as in Figure 17b. A many flat plate model is built by assuming each beam strikes a small plate whose area is the square of the beam separation distance. The small plate's orientation in space is drawn from adjacent photon beam lengths, as is the surface normal. Internal edges are estimated with a beam length difference threshold.

The pixel-based SRP force/moment model is compared to the flat plate model by sampling the force and torque across 180 degrees of yaw. For the comparison, the pixel model employs a 0.5 m pixel width. The resulting yaw vs torque profile for the flat plate model and the pixel model appear in Figure 18.

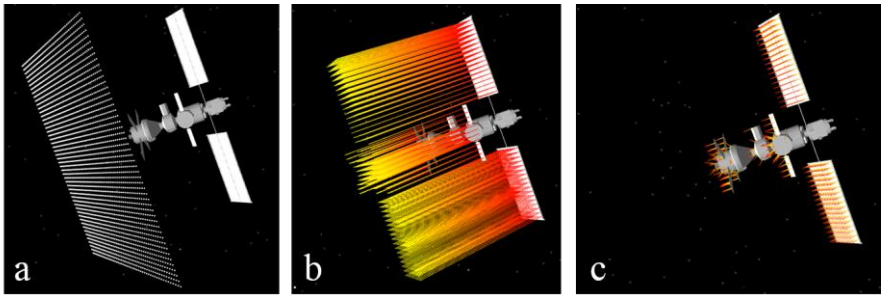

Figure 17. The photon plane (a). Photon beam strikes (b). Surface normals (c).

The two torque traces are similar in behavior and magnitude. The flat plate model's torque curve through yaw angles is continuous without noise, in contrast to the pixel model, whose torque curve has variations within the curve due to self-shadowing and plates popping in and out of existence as the spacecraft rotates underneath the photon plane. The two torque profiles have different maximum torque values which suggest the measurements of the flat plates don't fully capture the geometry of the spacecraft.

Nevertheless, the similarities between the very simple flat plate model and the individually-constructed pixel model are strong enough to consider the performance advantages of the flat plate model approximation. For the purposes of these analyses, the simplified flat plate model is used for computational speed. For future analyses of more transient events such as proximity operations and docking/undocking, the pixel model may be useful to capture the shadowing interactions between two spacecraft in proximity.

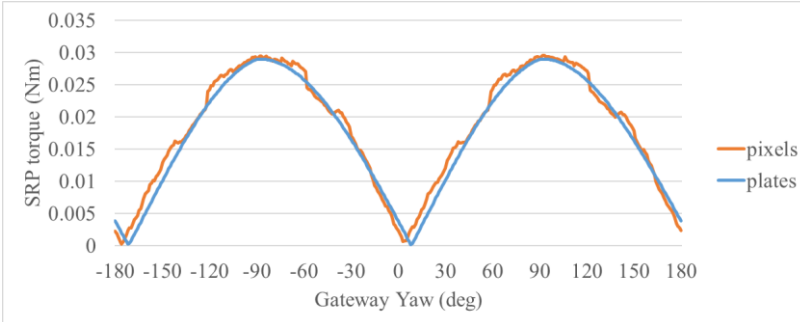

Figure 18. Yaw angle vs Torque for the flat plate model and pixel model with 0.5m resolution.

Attitude Control System Sizing and Performance

The Gateway attitude control system is housed in the PPE and contains a system of reaction wheels or CMGs (heretofore denoted "wheelset"), and a propulsive system of hydrazine fueled RCS thrusters. A central focus of the attitude studies is an investigation into sizing and performance of an attitude control system to satisfy Gateway requirements. The sizing and performance study has two goals, 1) to define the smallest wheelset that can feasibly handle the requirements of the mission and 2) estimate hydrazine propellant use rate for nominal operations of both uncrewed and crewed Gateway configurations.

A properly sized wheelset must function throughout the Gateway lifetime. The Gateway grows with additional components that add mass and angular inertia to the combined system and in turn reduce the command authority of the wheelset. A candidate wheelset must possess enough momentum storage and torque output to slew the Gateway from SPEA to the OMM direction and back within a specified time and without saturating the wheelset. As a matter of process, the wheelset is desaturated by command before an executed OMM sequence. Any desaturation triggered automatically from system momentum exceeding the maximum wheelset capacity is considered an "automatic" desaturation. If the wheelset is inadequately sized, automatic desaturations may occur frequently during slew execution (due to a slew rate too fast for the wheelset), during perilune passages (due to a gravity gradient too severe for the wheelset), or throughout a crewed revolution (due to venting too powerful for the wheelset). Frequent automatic desaturations in the simulation suggest the wheelset cannot handle either the perturbations or the slew speed; it is considered too small to feasibly control the Gateway.

The total wheelset momentum capacity is approximated as a spherical envelope over the body axes with a radius 1.633 times the momentum capacity of a single wheel. This approximation assumes four identical wheels mounted in an equilateral pyramid.[13] Torque capability is parallel to momentum capacity, so the available torque in the body frame is also a sphere of radius 1.633 times the torque of a single wheel. For example, the baseline reaction wheel is assumed to have a capacity of 250 Nms, so the total momentum capacity of a pyramid of four baseline wheels will have a system capacity of 408 Nms. The theoretical maximum slew rate of the stack is defined as the slew rate achieved when the wheels are commanded from zero momentum to saturation along the axis of rotation of the largest principal moment of inertia. This maximum slew rate represents a bound below which the stack can slew to any direction without saturating the wheels. Maximum slew rates for three sample wheelsets appear in Table 8 for six gateway configurations. Of course, stacks characterized by larger principal moments of inertia have significantly slower maximum slew rates. Assuming each wheelset operates at its theoretical maximum slew rate, the time in minutes to slew 180° along the largest MOI for each configuration and wheelset pair also appear in Table 8. If the goal is to slew in under an hour, the smallest wheelset is only appropriately sized for the smallest uncrewed stacks, configurations 1 and 3. The largest wheelset can slew all but the largest crewed configuration 180° within about an hour.

To calculate the propellant use for desaturations during uncrewed operations, configurations 1, 3, 5 and 7 are each simulated with each wheelset and associated maximum slew rate. In the uncrewed analysis, the Gateway orbits in the 9:2 LSR NRHO and performs OMMs at apolune as necessary to maintain orbit. Prior to each OMM, the Gateway slews to the maneuver attitude using CMGs/wheels. After the OMM is performed using SEP thrusters, a new SPEA is targeted and the Gateway slews to its new attitude. Throughout, errors in attitude, SRP, navigation, and maneuver execution are applied as specified in Table 2. Year-

long uncrewed simulations are executed in a Monte Carlo process to investigate feasibility and behavior of the Gateway in response to different configurations, noise and perturbation values, and attitude control processes and events. The simulations track the propellant use for OMMs and momentum desaturations as a function of the input control system, gateway configuration, and error values.

Table 8. Maximum slew rates and time to perform a 180 degree slew for various configurations

Config	Analysis baseline 408 Nms		Honeywell M600 1328 Nms		Honeywell M1400 3099 Nms	
	Max rate (deg/s)	Slew time (min)	Max rate (deg/s)	Slew time (min)	Max rate (deg/s)	Slew time (min)
1	0.097	30.8	0.316	9.5	0.732	4.1
2	0.015	205.3	0.048	63.1	0.111	27
3	0.057	52.6	0.185	16.2	0.435	6.9
4	0.010	295.2	0.033	90.7	0.077	38.9
5	0.003	1193.5	0.008	366.7	0.019	157.1
6	0.006	487.7	0.020	149.8	0.047	64.2

In Table 9, the number of desaturations per revolution and the associated mean annual hydrazine propellant used in kg per year for each uncrewed configuration and wheelset is given for 50 Monte Carlo trials per case. For configurations 1 and 3, only a single desaturation per revolution is commanded prior to the OMM; the solar/gravity torques do not saturate the wheelset during the orbit. As the Gateway stack grows, the number of desaturation events per revolution grows significantly and there is a distinct increase in propellant used per year. This is due to the gravity gradient torques over the periapsis of the Moon repeatedly saturating the undersized wheelset and triggering sequential momentum desaturation maneuvers. The Gateway stack increases in length and maintains a SPEA that induces significant gravity gradient torques near perilune.

There are several ways to mitigate the excessive propellant use and desaturation rate from gravity gradient torques on larger stacks. One is to adjust the stack attitude, turning away from SPEA during perilune passages to an orientation that minimizes the gravity torques; analysis is ongoing. Additionally, the Gateway is modular, so reconfiguration to reduce the moment of inertia is another effective option. In configuration 7, the major components are all mounted inline, with only an LE in a radial position, as pictured in Figure 19a. If a second module is also mounted radially instead of axially, as in Figure 19b, the total stack length is reduced by 8 m and the largest principal moment of inertial is reduced by about 35%. The resulting configuration 7b is denoted the “cross stack” for its appearance. Results from a one-year simulation appear in the final row of Table 9. Though identical in mass to configuration 7, the cross stack requires less than half the hydrazine propellent for a year of desaturation events.

Table 9. Desaturation frequency and mean annual hydrazine use for uncrewed attitude control

Config	Analysis baseline 408 Nms		Honeywell M600 1328 Nms		Honeywell M1400 3099 Nms	
	desats per rev	annual hydrazine (kg)	desats per rev	annual hydrazine (kg)	desats per rev	annual hydrazine (kg)
1	1.0	2.4	1.0	2.4	1.0	1.9
3	1.0	1.0	1.0	1.5	1.0	3.3
4	4.6	29.9	1.7	26.5	1.0	8.1
6	7.7	37.7	2.6	32.6	1.4	28.4
6b	3.9	19.7	1.6	16.6	1.77	

Attitude Maintenance: Crewed Configurations

During crewed revolutions, the ACS is more highly taxed because of the added mass/inertia of the Orion spacecraft, the docking perturbations, and venting from Orion. Attitude is maintained through docking and venting instances, and the angular momentum imparted by each event is absorbed by the wheelset. As in the OM analysis, two docking scenarios are considered. The first scenario starts with four revolutions of the initial uncrewed configuration 1 from Table 1. An Orion docking event transitions the Gateway from configuration 1 to 2. The Gateway remains in a crewed configuration 2 for one full revolution before un-

docking to shift to configuration 3. This final configuration is maintained for ten revolutions until the OMM behavior settles to a steady state. Throughout the simulation, errors are applied as specified in Table 2. The simulated crewed scenario is run for each Sun-Moon-Gateway geometry for 50 Monte Carlo trials each. The number of desaturation events per rev is computed, as well as the hydrazine cost for the duration of the crewed visit. Results appear in Table 10.

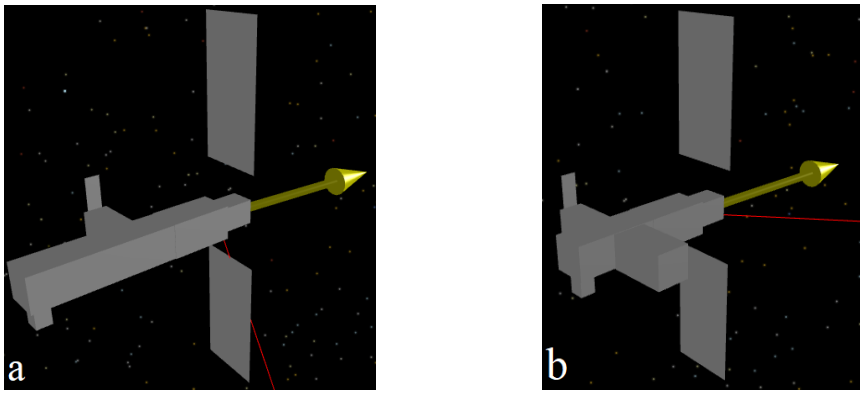

Figure 19. Flat plate model representing configuration 7 (a) and the cross-stack (b)

Perturbations have a larger effect on smaller configurations, but larger configurations are more affected by gravity gradient torques and are more difficult to control with the same attitude control system. To explore this concept, a second docking simulation explores a larger set of configurations. It commences with four revolutions in the uncrewed configuration 5 from Table 1. Orion docks and spends four full revolutions at the gateway in crewed configuration 6, the largest stack explored. After undocking, the simulation continues for 10 revolutions in the uncrewed configuration 7. Again, 50 Monte Carlo trials are run to assess the attitude control behavior, and the desaturation frequency and hydrazine cost for the crewed stay are recorded. Results appear in Table 10.

Table 10. Desaturation frequency and hydrazine use for attitude control: docking scenarios

Config	Desaturations Per Revolution		RCS Fuel Used Per Revolution	
	Mean	Max	Mean	Max
2	120.8	123.4	21.1	21.6
6	120.4	130.1	27.2	29.9

Note that the desaturation count and fuel use per revolution are notably similar despite significantly different sizes and shape of gateway stacks. The reason for this is tradeoff of CO_2 puffing and increased gravty gradient torques. Configuration 6 does not see CO_2 puffing from the Orion spacecraft as a habitat element is assumed to handle air regulation without venting that would torque the system. However, configuration 6 is longer and more susceptible to gravity gradient torques. While configuration 2 vents and desaturates somewhat consistently through its revolution, configuration 6 has its momentum desaturations clustered around perilune as it attempts to reject momentum built up from gravity gradient.

SUMMARY AND CONCLUDING REMARKS

As the Gateway is constructed over time in components, operations will include stretches of quiet, uncrewed operations as well as docking events followed by crewed revolutions within the NRHO. Orbit maintenance, orbit determination, and attitude control must be reliable and within propellant budget throughout all mission phases.

The total xenon budget from an OMM/Attitude perspective (that is, not including Gateway transfers or excursions to other orbits) must only consider uncrewed orbit maintenance burns. The total hydrazine budget is more complicated; it must account for desaturations throughout the Gateway lifetime, as well as slews and OMMs during crewed operations. The cost depends on Gateway configuration, errors incident on the spacecraft, OD accuracy, duration of crew residence at the Gateway, solar orientation at docking, and other factors such as the selected wheelset. The Orion tail-to-Sun requirement has a significant effect on the

hydrazine budget, both by constraining Gateway attitude and by necessitating slews and OMMs to be performed by the RCS thrusters.

In spite of frequent desaturations and venting during crewed operations, radiometric DSN tracking can maintain OD knowledge of the Gateway position and velocity to meet requirements that allow low-cost OM. With careful placement of DSN passes, requirements can be met without needing continuous tracking.

Future work includes the investigation of alternate attitudes near perilune to mitigate gravity gradient torques and the further exploration of other primary orbits that may offer advantages for OM, OD, or attitude control, for example a 4:1 LSR NRHO. Autonomous OD is of interest and is under investigation.

ACKNOWLEDGMENTS

The authors would like to thank Ryan Sieling for his insight and confirmation of the attitude analysis. Part of the research described in this paper was performed at the Jet Propulsion Laboratory, California Institute of Technology, under contract with the National Aeronautics and Space Administration. Part of the research described in this paper was performed at Johnson Space Center under contract #NNJ13HA01C.

REFERENCES

[1] Zimovan, E., K. C. Howell, and D. C. Davis, "Near Rectilinear Halo Orbits and Their Application in Cis-Lunar Space," 3rd IAA Conference on Dynamics and Control of Space Systems, Moscow, Russia, May-June 2017.

[2] Davis, D. C., S. A. Bhatt, K. C. Howell, J. Jang, R. L. Whitley, F. D. Clark, D. Guzzetti, E. M. Zimovan, and G. H. Barton, "Orbit Maintenance and Navigation of Human Spacecraft at Cislunar Near Rectilinear Halo Orbits," 27th AAS/AIAA Space Flight Mechanics Meeting, San Antonio, Texas, February 2017.

[3] Guzzetti, D., E. M. Zimovan, K. C. Howell, and D. C. Davis, "Stationkeeping Methodologies for Spacecraft in Lunar Near Rectilinear Halo Orbits," AAS/AIAA Spaceflight Mechanics Meeting, San Antonio, Texas, February 2017.

[4] Davis, D. C., S. M. Phillips, K. C. Howell, S. Vutukuri, and B. P. McCarthy, "Stationkeeping and Transfer Trajectory Design for Spacecraft in Cislunar Space," AAS/AIAA Astrodynamics Specialists Conference, Stevenson, Washington, August 2017.

[5] Whitley, R. and R. Martinez, "Options for Staging Orbits in Cislunar Space," IEEE Aerospace 2015, Big Sky Montana, March 2015.

[6] Whitley, R.J., D.C. Davis, M.L. McGuire, L.M. Burke, B.P. McCarthy, R.J. Power, K.C. Howell, "Earth-Moon Near Rectilinear Halo and Butterfly Orbits for Lunar Surface Exploration", AAS/AIAA Astrodynamics Specialists Conference, Snowbird, Utah, August 2018.

[7] Pritchett, R., E. Zimovan, and K. C. Howell, "Impulsive and Low-Thrust Transfer Design between Stable and Nearly Stable Periodic Orbits in the Restricted Problem," 18th AIAA SciTech Forum, Kissimmee, Florida, Jan 2018.

[8] Lantoine, G. "Efficient NRHO to DRO transfers in cislunar space", AAS/AIAA Astrodynamics Specialists Conference, Stevenson, Washington, August 2017.

[9] Williams, J., D. E. Lee, R. L. Whitley, K. A. Bokelmann, D. C. Davis, and C. F. Berry, "Targeting Cislunar Near Rectilinear Halo Orbits for Human Space Exploration," 27th AAS/AIAA Space Flight Mechanics Meeting, San Antonio, Texas, February 2017.

[10] D'Souza, C. and G. Barton, "Process Noise Assumptions for Orion Cislunar Missions," NASA MPCV Technical Brief, August 2016.

[11] D. Folta, T. Pavlak, K. Howell, M. Woodard, and D. Woodfork, "Stationkeeping of Lissajous Trajectories in the Earth-Moon System with Applications to ARTEMIS," 20th AAS/AIAA Space Flight Mechanics Meeting, Feb. 2010.

[12] J. Petersen and J. Brown, "Applying Dynamical Systems Theory to Optimize Libration Point Orbit Stationkeeping Maneuvers for WIND," AAS/AIAA Astrodynamics Specialists Conference, Aug. 2014.

[13] Markley, F.L., R.G. Reynolds, F.X. Liu, and K.L. Lebsock, "Maximum torques and momentum envelopes for reaction-wheel arrays," Journal of Guidance, Control, and Dynamics, Vol. 33, No. 5, 2010.